



**EUROfusion**

WPENS-CPR(17) 17554

V Hauer et al.

## **IFMIF-DONES gas flow modelling**

Preprint of Paper to be submitted for publication in Proceeding of  
13th International Symposium on Fusion Nuclear Technology  
(ISFNT)



This work has been carried out within the framework of the EUROfusion Consortium and has received funding from the Euratom research and training programme 2014-2018 under grant agreement No 633053. The views and opinions expressed herein do not necessarily reflect those of the European Commission.

This document is intended for publication in the open literature. It is made available on the clear understanding that it may not be further circulated and extracts or references may not be published prior to publication of the original when applicable, or without the consent of the Publications Officer, EUROfusion Programme Management Unit, Culham Science Centre, Abingdon, Oxon, OX14 3DB, UK or e-mail [Publications.Officer@euro-fusion.org](mailto:Publications.Officer@euro-fusion.org)

Enquiries about Copyright and reproduction should be addressed to the Publications Officer, EUROfusion Programme Management Unit, Culham Science Centre, Abingdon, Oxon, OX14 3DB, UK or e-mail [Publications.Officer@euro-fusion.org](mailto:Publications.Officer@euro-fusion.org)

The contents of this preprint and all other EUROfusion Preprints, Reports and Conference Papers are available to view online free at <http://www.euro-fusionscipub.org>. This site has full search facilities and e-mail alert options. In the JET specific papers the diagrams contained within the PDFs on this site are hyperlinked

# IFMIF-DONES gas flow modelling

V. Hauer, Chr. Day

Karlsruhe Institute of Technology (KIT), Karlsruhe, Germany

## Abstract

Simulations of the gas flow inside the IFMIF-DONES vacuum system were performed with Molflow+. The IFMIF-DONES model is based on the last IFMIF-EVEDA design and of the LIPAc accelerator, which is being built for testing IFMIF accelerator components. Both, LIPAc and IFMIF-DONES share the same accelerator subsystems. The model was prepared for simulation by adding different sets of boundary conditions for the pumping of deuterium and hydrogen caused by beam losses and outgassing, respectively. A model of the lithium target was set up to study the lithium condensation at beamline components.

The simulations of lithium layer deposition in the vacuum system show no degradation of the vacuum performance. The simulations of the gas pumping show pressure profiles which are mainly caused by the beam losses in this subsection. In general, the pressure profiles of the different subsections are nearly independent from each other caused by the small apertures installed between the subsections.

Keywords: IFMIF; DONES; beamline; vacuum;

## 1. Introduction

IFMIF, the International Fusion Materials Irradiation Facility, is a test facility for materials foreseen in fusion reactors. High neutron fluxes are generated with energy spectrum and intensity similar to the conditions at the burn phase inside a fusion reactor. The high energy neutrons are generated by accelerating deuterons onto a lithium target. IFMIF-EVEDA (Engineering Validation and Engineering Design Activities) includes two beamlines with a beam current of 125 mA each [1]. IFMIF-DONES (DEMO-Oriented Neutron Source) will be similar to IFMIF-EVEDA but will only have one accelerator [2].

Each IFMIF beamline consists of different subsections: one Electron Cyclotron Resonance (ECR) ion source, one Low Energy Beam Transport (LEBT) section, one Radio Frequency Quadrupole (RFQ), one Medium Energy Beam Transport Line (MEBT), four Superconducting Radio Frequency Linac (SRF-LINAC) modules, one High Energy Beam Transport Line (HEBT) and one Beam dump (BD) (see Fig. 1). The lithium target (LT) has connections to one or two beamlines depending on the IFMIF design [1].

The LIPAc (Linear IFMIF Prototype Accelerator system) is a test bed for validation of accelerator components of the IFMIF-DONES accelerator. It is in commissioning phase now and will be operated in the next couple of years. The subsection arrangement is very similar to the one of the IFMIF beamline except that there is only one SRF-LINAC module included. The

lithium target (LT) is not part of LIPAc [3]. It is tested at the EVEDA Lithium Test Loop [4].

## 2. Simulation tools

The simulations were done by the TPMC (Test Particle Monte Carlo) method. This approach neglects the inter-particle collisions and is based on ray tracing of the particle trajectories with a high number of simulated particles in order to achieve good statistics. The solutions obtained by TPMC allow the calculation of all quantities based on particle density. The pressure on a surface can be directly computed by the counted particle density and the mean value of the temperature of these particles.

The simulated particles are generated at those surfaces which are defined as source. Typically, the sources are simulating particle inflow, beam losses or thermal outgassing. For the calculations shown here, diffuse reflection has been assumed, both for the source terms and for the particle reflections at the surfaces. If a test particle hits a pumping surface it will be deleted with a probability proportional to the given sticking factor of this surface. The sticking factor is calculated as the ratio of pumped particles to the number of impinging particles.

The total number of generated test particles and the hits on all surfaces are counted. Moreover, all surfaces are covered by a mesh with a typical mesh size of 10 by 10 mm to increase the resolution of particle density calculation. Molflow+ version 2.6.19 and 2.49 were used

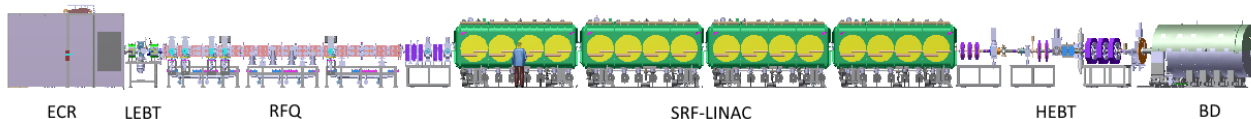


Fig. 1: picture of the IFMIF accelerator.

for all simulations. Molflow+ is a Monte Carlo code developed at CERN by R. Kersevan and M. Ady [5].

### 3. Simulation models

The simulation models were generated from CAD models of the IFMIF-EVEDA and LIPAc accelerator and the lithium target system.

In a first step the vacuum relevant parts of the overall CAD model were extracted. Components which are not part of the vacuum system were deleted. In a second step, details of the vacuum parts were replaced by simplified parts. The reduced CAD models were converted to the input format needed for the simulation software Molflow+. This procedure is exemplified in Fig. 2 which shows the extracted, the simplified and the reduced CAD model of the HEBT including the beam dump.

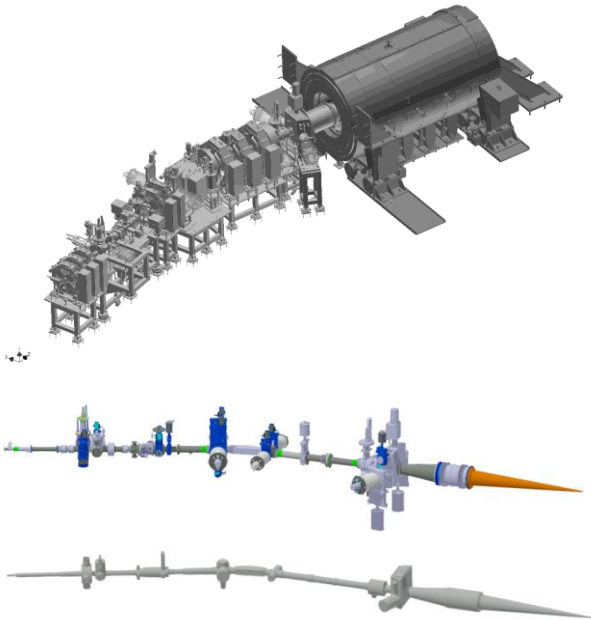


Fig. 2: Extracted (top), simplified (middle) and reduced (bottom) CAD model of HEBT and beam dump.

The submodels, except the subsection model of the lithium target (see Fig. 3) were combined to more complex models for the sections LEBT-RFQ-MEBT and HEBT-BD. Both sections are characterized by large beam losses at the end of LEBT and the second and third section of RFQ as well as inside the beam dump, respectively.

The section models were combined with four SRF-LINAC modules to the IFMIF-EVEDA beam line



Fig. 4: Geometrical representation of the IFMIF-DONES simulation model (taken from MOLFLOW+).

model. After that the IFMIF-EVEDA model was modified to represent the latest IFMIF-DONES beamline design (see Fig. 4). The main differences of both IFMIF models are the changed configuration of magnets and cavities of the SRF-LINAC modules 2 to 4 to guarantee the required beam particle energy.

Simulations were performed with the section models (LEBT-RFQ-MEBT, HEBT-BD) and the IFMIF-DONES model, respectively.



Fig. 3: Geometrical representation of the lithium target simulation model (taken from MOLFLOW+).

### 4. Calculation of pressure and particle density

Pressures and particle densities were calculated in two different ways: based on the hits onto special counting surfaces included in the models and as mean value of the values at all inner surfaces.

In the first way transparent surfaces were placed in the centreline of the models which count the hits of particles without affecting the particle tracks themselves. Based on the hits the neutral particle densities can be calculated in or close to the beam axis. These numbers give an estimation of the neutral particles which interact with the beam.

In a second way the mean property values of particle density and pressure were calculated in slices along the beamline axis with a slice thickness of the size of one mesh cell. For example, if  $z$  is the coordinate along the beamline axis, the property values of all cells which are positioned between  $z_i$  and  $z_{i+1}$  were summed up and divided by the total number of cells. The difference between  $z_{i+1}$  and  $z_i$  is the size of one mesh cell (10 mm).

The total number of cells in one slice differs along the beamline and depends on the geometrical shape of model. The calculated mean values give an estimation of particle densities and pressures can be measured with pressure sensors attached at the beamline vacuum system.

## 5. Boundary conditions for simulations

### 5.1 Gas compositions

The neutral gas composition is mainly dominated by deuterium at beam operation caused by the beam losses at LEBT, RFQ and beam dump (at beginning of operation). After the beam start-up is completed, the deuterons will mainly be absorbed at the liquid lithium target. The effective vapor pressure of lithium at 570 K in combination with the high flow speed and curvature of the target results in values of about  $10^{-5}$  mbar. Therefore lithium steam is the dominant gas species close to the target. The temperature gradient along the beam ducts connected to the target leads to a condensation of the lithium at these surfaces. The partial pressure of lithium decreases very rapidly with the distance from the target.

Gas compositions, operating pressures and temperatures at LIPAc and LT components (see Table 1) were extracted from unpublished former work inside the framework of the EUROfusion Consortium and [6-8]. Identical gas compositions and pump systems were assumed for IFMIF-DONES subsystems.

Table 1. Gas compositions, pressures and temperatures at the different subsections of LIPAc and IFMIF-DONES.

	Composition	Pressure (mbar)	Temperature (K)
<b>LEBT</b>	D <sub>2</sub> , Kr	$1 \cdot 10^{-5}$ D <sub>2</sub>	300
	+outgassing	$4 \cdot 10^{-5}$ Kr	
<b>RFQ</b>	D <sub>2</sub> ,	$< 5 \cdot 10^{-7}$	290-340
	+outgassing		
<b>MEBT</b>	D <sub>2</sub> ,	$5 \cdot 10^{-7}$	300
	+outgassing	$-5 \cdot 10^{-8}$	
<b>SRF-L</b>	D <sub>2</sub> ,	$< 5 \cdot 10^{-8}$	4.4-300
	+outgassing		
<b>HEBT</b>	D <sub>2</sub> ,	$< 5 \cdot 10^{-8}$	300
	+outgassing	(SRF side)	
<b>BD</b>	D <sub>2</sub> ,	$3 \cdot 10^{-6}$	>300
	+outgassing		
<b>LT</b>	D <sub>2</sub> +	$10^{-5}$	300-570
	outgassing + Li steam + product of Li/d reaction	(at free-surface)	

### 5.2 Outgassing

The gas composition of the beamline vacuum systems without beam operation is given by thermally desorbed gas from the inner surfaces. The vacuum parts of IFMIF-DONES will be mainly produced from stainless steel, copper and niobium. The residual gas atmosphere is assumed to be mainly composed of hydrogen. The outgassing of the different parts is dependent on the used material and conditioning but also from the history starting with the production of the materials. Therefore the resulting outgassing rates can

vary in the range of several orders of magnitude [9]. The values for hydrogen outgassing from pre-baked stainless steel, OFHC and electroplated copper (see Table 2) were extracted from former work inside the framework of the EUROfusion Consortium. The niobium surfaces are assumed to be nearly saturated with one monolayer of hydrogen at a temperature of 4.5 K. Therefore the outgassing as well as pumping by the niobium surfaces is mainly neglected [10].

Table 2: Outgassing rates for hydrogen used in simulations.

	Outgassing rates for hydrogen (mbar·l/s·cm <sup>2</sup> )
<b>AISI 316L</b>	$3.87 \cdot 10^{-11}$
<b>OFHC Copper</b>	$2.31 \cdot 10^{-13}$
<b>Electroplated copper</b>	$1.71 \cdot 10^{-10}$

### 5.3 Beam losses

Gas loads were extracted from former work inside the framework of the EUROfusion Consortium. They are calculated under the assumption of a complete recombination of the deuterium ions to molecules at the surface.

The beam losses at LEBT are assumed to be uniformly distributed along the injection cone before the RFQ section. The beam losses inside the RFQ are simulated by outgassing of four flat surfaces located near the RFQ pole tips with a cosine angular distribution. Because the losses are distributed along the RFQ with different intensity (see Fig. 5), a discrete outgassing map is implemented for every of the four tips in the simulation model. Equally distributed beam losses are assumed along the beamline tube of MEBT and HEBT whereas concentrated beam losses are assumed on the first scrapers of MEBT and inside the beam dump. Table 3 summarizes the gas loads by thermal outgassing and beam losses.

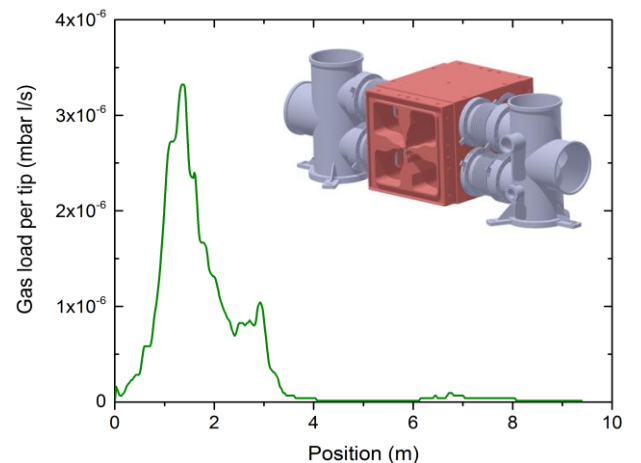


Fig. 5: Gas load per tip along the position inside the RFQ caused by beam losses (taken from unpublished former work).

Table 3: Gas loads in the different subsections of IFMIF-DONES.

	Thermal outgassing $\left(\frac{\text{mbar l}}{\text{s}}\right)$	Beam losses $\left(\frac{\text{mbar l}}{\text{s}}\right)$
<b>LEBT</b>	$8.3 \cdot 10^{-7}$	$7.8 \cdot 10^{-3}$
<b>RFQ</b>	$5.2 \cdot 10^{-6}$	$1.2 \cdot 10^{-3}$
<b>MEBT</b>	$3.8 \cdot 10^{-6}$	$7.6 \cdot 10^{-5}$
<b>SRF-L</b>	0	0
<b>HEBT</b>	$3.7 \cdot 10^{-6}$	$2.3 \cdot 10^{-8}$
<b>BD</b>	$2.0 \cdot 10^{-6}$	$1.6 \cdot 10^{-2}$

## 5.4 Pumping speeds

The pumps are represented in the models by pumping surfaces with a certain sticking factor. The pumping speeds are usually given for different gases (e.g. hydrogen and nitrogen) by the manufacturers, which were used for the calculations of sticking factors for these gases. If the pumping speed for a gas is not known (e.g. deuterium) the pumping speeds have to be estimated depending on the used pump type.

Turbomolecular pumps (TMP) show in general a slightly increasing pumping speed with increasing molar mass for lighter gases, but the quantitative difference of the pumping speed for  $\text{H}_2$  and  $\text{D}_2$  is not accurately known for the used pumps. A conservative approach is hence employed which assumes identical pumping speeds for hydrogen and deuterium; this means whilst the sticking factors varied for the gases.

Capture pumps like cryopumps (CP), ion pumps (IP) and titan sublimation pumps (TiSP) show a decreasing pumping speed with increasing molar mass. Here, the pumping speed is assumed to vary with the square root of molar mass whilst the sticking factor has been kept constant. Also this is a relative conservative approach. Table 4 summarizes pump types, pumping speeds and sticking factors for hydrogen used in the gas flow simulation of IFMIF-DONES. For convergence reasons, a sticking factor of 0.001 was chosen for the inner surfaces of the SRF-LINAC modules to avoid endless reflections of particle insides this subsections.

## 6 Simulation results

### 6.1 Gas flow in IFMIF-DONES

The IFMIF-DONES model combines the subsection models of LEBT, RFQ, MEBT, SRF-LINAC module 1 to 4 and HEBT including the beam dump (see Fig. 4). Gas loads are assumed as combination of thermal outgassing and beam losses (see Table 3).

Different TPMC simulations were performed for beam losses (particle molar mass = 4) and thermal outgassing (particle molar mass = 2), respectively. Fig. 6 shows the resulting gas pressure profile for the subsections LEBT, RFQ and MEBT. The gas pressure profile reflects directly the distribution of gas loads caused by beam losses. The high gas loads at the end of LEBT (cone), the

third and fourth module of RFQ and the entrance of MEBT (first scraper) are represented as pressure peaks in the profile. The small apertures between the subsections decouple the pressure distribution inside the subsections from each other which can be seen by the large pressure drop at the end of LEBT and the pressure increase at the entrance of MEBT.

Table 4: Pump type, pumping speed and sticking factor for hydrogen at the different subsections of LIPAc and IFMIF-DONES.

	Pump	Pumping speed for hydrogen (l/s)	Sticking factor
<b>LEBT</b>	TMP 1	2100	0.10
	TMP 2	115	0.09
<b>RFQ</b>	CP 1–10	2200	0.15
	IP 1–4	525	0.04
<b>MEBT</b>	TMP 1–3	510	0.06
	IP (+ TiSP)	875 (1800)	0.11 (0.22)
<b>SRF-LINAC</b>	none	pre-evacuated at $10^{-7}$ mbar	0.001
<b>HEBT</b>	CP 1–2	5000	0.24
	CP 3	1500	0.20
	IP 1 (+ TiSP)	875 (1800)	0.14 (0.30)
	IP 2 (+TiSP)	260 (1250)	0.08 (0.37)
<b>BD</b>	none	pumped by HEBT	0
<b>LT</b>	TMP 1	5000	0.06
	TMP 2	400	0.08

Fig. 7 shows the calculated gas pressure profile for the subsections HEBT and beam dump. The pressure profile is smoother caused by the large opening between HEBT and beam dump which results in a good communication between the two sub-systems. The beam losses at the beam dump contribute the highest amount to the total gas load which leads to high pressures inside this subsection. The large pressure drop between beam dump and end of SRF-LINAC is caused by large cryopumps installed at HEBT to guarantee the low pressure which is required for operation of the SRF-LINAC.

### 6.2 Simulation of lithium target performance

The simulations of the lithium condensation close to the target were performed including the target chamber and the beamline vacuum system up to the HEBT. The interactions of the lithium vapor with the beam and residual gas are neglected in this case. The aim of these simulations is to get values of the lithium layer deposition for different areas of beamline components close to the target. The boundary conditions for this case were extracted from former work inside the framework of the EUROfusion Consortium and are summarized in Table 5. Fig. 3 shows the volume model used in MOLFLOW+.

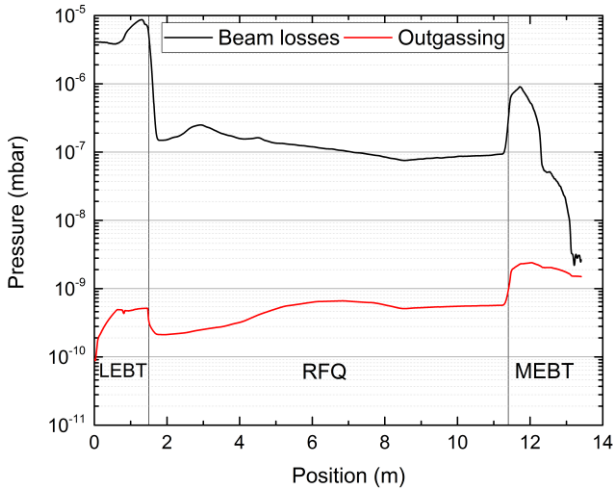


Fig. 6: Gas pressure profile in the LEBT-RFQ-MEBT section. The vertical lines indicate the positions of the interfaces between the IFMIF-DONES subsections.

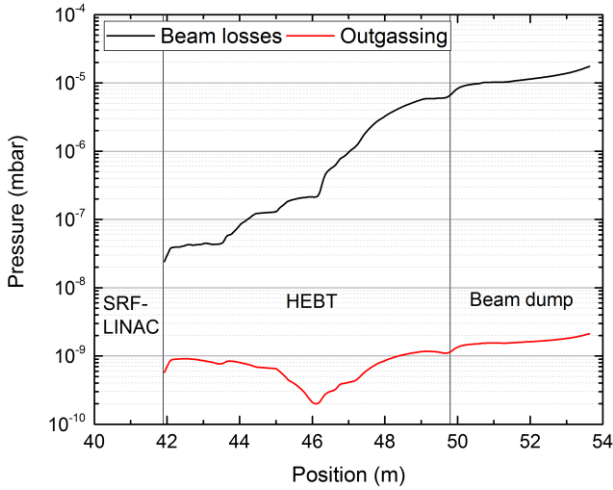


Fig. 7: Gas pressure profile in the HEBT and beam dump subsection. The vertical lines indicate the positions of the interfaces between the three subsections.

Table 5: Boundary conditions for simulation of lithium condensation.

Fluid	Lithium vapor
Fluid temperature	523 K
Fluid pressure	$10^{-5}$ mbar
Sticking factor	1
Surface temperature	293 K

The rate of adsorbed particle and the layer thickness of condensed lithium onto the inner surface at one year of operation were calculated assuming 200 operation days (8 hours per day). The results are plotted in Fig. 8. The gaps in the graph are caused by no hits in these parts of the model. This area is shadowed due to cross section changes.

The layer thickness decreases rapidly with the distance from the target. Nevertheless the lithium layer thickness at surfaces close to the target can reach several millimeters in one year. The peaks in the graph indicate higher values

of lithium deposition caused by cross section reduction at this point.

In summary, the vacuum performance will not be influenced as long as the total outgassing rate is not increased by the deposited layer (sum of total outgassing rate) or the pump performance is not degraded by condensation of lithium inside the pumps.

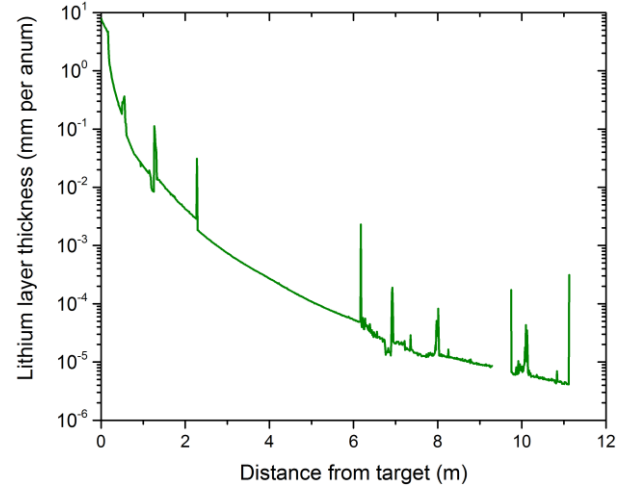


Fig. 8: Lithium layer thickness in dependence on the distance from the target (target pressure of  $10^{-5}$  mbar).

## 6. Conclusion and Outlook

The simulation of gas flows inside the IFMIF-DONES beamline vacuum system shows pressure profiles which are mainly caused by the beam losses in this subsection. The pressure profiles of the different subsections are nearly independent from each other caused by the small apertures installed between these subsections. Future work will include simulations of the IFMIF-DONES accelerator system coupled with the EVEDA target system.

The lithium layer deposition in the vacuum system close to target has most probably no degradation effect onto the vacuum performance. Nevertheless, the effects of lithium condensation on outgassing and installed equipment (e.g. pumps, pressure sensors, beam diagnostics) have to be checked in future.

## Acknowledgments

This work has been carried out within the framework of the EUROfusion Consortium and has received funding from the Euratom research and training programme 2014-2018 under grant agreement No 633053. The views and opinions expressed herein do not necessarily reflect those of the European Commission.

## References

- [1] IFMIF Intermediate Engineering Design Report, BA\_D\_2MR6YQ, version 1.0 (2013).
- [2] A. Ibarra, et al., A stepped approach IFMIF/EVEDA towards IFMIF, Fusion Sci. Technol., 66 (2014),

252-259.

- [3] <http://accelconf.web.cern.ch/AccelConf/ipac2016/papers/mozb02.pdf>
- [4] H. Kondo, et al., Demonstration of Li target facility in IFMIF/EVEDA project: Li target stability in continuous operation of entire system, Fus. Eng. Des., 109–111 (2016) 1759–1763.
- [5] <http://molflow.web.cern.ch/>
- [6] [http://accelconf.web.cern.ch/AccelConf/e08/papers/thpp078.pdf#search=domain%3Daccelconf.web.cern.ch%2Bauthor%3A"pisent" url%3Aaccelconf%2Fe08FileExtension%3Dpdf -url%3Aabstract -url%3Aaccelconf%2Fjacow](http://accelconf.web.cern.ch/AccelConf/e08/papers/thpp078.pdf#search=domain%3Daccelconf.web.cern.ch%2Bauthor%3A) .
- [7] <https://accelconf.web.cern.ch/accelconf/IPAC2011/papers/weps058.pdf>.
- [8] <https://accelconf.web.cern.ch/accelconf/IPAC2013/papers/thpfi003.pdf> .
- [9] K. Battes et al., Outgassing rate measurements of stainless steel and polymers using the difference
- [10] Method, J. Vac. Sci. Technol., A 33, 2 (2015).
- [11] M. A. Pick, M. G. Greene, The sticking coefficient of hydrogen on niobium, Surface Science 93 (1980), 129-134.